ORIGINAL ARTICLE

Inhibition of myostatin in mice improves insulin sensitivity via irisin-mediated cross talk between muscle and adipose tissues

J Dong[1,2,4], Y Dong[2,3,4], Y Dong[2], F Chen[1], WE Mitch[2] and L Zhang[2]

BACKGROUND/OBJECTIVE: In mice, a high-fat diet (HFD) induces obesity, insulin resistance and myostatin production. We tested whether inhibition of myostatin in mice can reverse these HFD-induced abnormalities.
SUBJECTS/METHODS: C57BL/6 mice were fed a HFD for 16 weeks including the final 4 weeks some mice were treated with an anti-myostatin peptibody. Body composition, the respiratory exchange ratio plus glucose and insulin tolerance tests were examined. Myostatin knock down in C2C12 cells was performed using small hairpin RNA lentivirus. Adipose tissue-derived stem cells were cultured to measure their responses to conditioned media from C2C12 cells lacking myostatin, or to recombinant myostatin or irisin. Isolated peritoneal macrophages were treated with myostatin or irisin to determine whether myostatin or irisin induce inflammatory mechanisms.
RESULTS: In HFD-fed mice, peptibody treatment stimulated muscle growth and improved insulin resistance. The improved glucose and insulin tolerances were confirmed when we found increased muscle expression of p-Akt and the glucose transporter, Glut4. In HFD-fed mice, the peptibody suppressed macrophage infiltration and the expression of proinflammatory cytokines in both the muscle and adipocytes. Inhibition of myostatin caused the conversion of white (WAT) to brown adipose tissue, whereas stimulating fatty acid oxidation and increasing energy expenditure. The related mechanism is a muscle-to-fat cross talk mediated by irisin. Myostatin inhibition increased peroxisome proliferator-activated receptor gamma, coactivator 1α expression and irisin production in the muscle. Irisin then stimulated WAT browning. Irisin also suppresses inflammation and stimulates macrophage polarization from M1 to M2 types.
CONCLUSIONS: These results uncover a metabolic pathway from an increase in myostatin that suppresses irisin leading to the activation of inflammatory cytokines and insulin resistance. Thus, myostatin is a potential therapeutic target to treat insulin resistance of type II diabetes as well as the shortage of brown/beige fat in obesity.

International Journal of Obesity (2016) **40,** 434–442; doi:10.1038/ijo.2015.200

INTRODUCTION

Myostatin, a myokine protein, is a member of transforming growth factor (TGF)-β superfamily. It is mainly expressed in skeletal muscle but is also detectable in cardiac muscle, blood and to a limited extent in adipose cells. Myostatin is considered to be a negative regulator of the growth of skeletal muscles, which has been intensively studied since it was found that the inactivation of the *myostatin* gene in mice or its mutation in cattle, sheep or humans accelerates muscle growth.[1–5] Contrariwise, myostatin expression in catabolic conditions can lead to muscle wasting.[6] Recent studies indicate that the influence of myostatin extends beyond influencing muscle growth: over expression of myostatin in mice causes insulin resistance, whereas genetic deletion of myostatin prevents obesity even though myostatin is expressed at a low level in adipose tissues.[7–9] In fact, adipose tissue-specific deletion of myostatin did not change muscle weight, body composition or glucose and insulin tolerance in mice fed a high-fat diet (HFD).[10] In contrast, whole-body myostatin knockout (KO) in mice fed normal chow or a HFD caused a significant reduction in total body adipogenesis and a lower level of serum leptin.[8] Moreover, whole-body myostatin deletion in mouse models of obesity (agouti lethal

yellow or leptin deficient, Lep[ob/ob], mice) has been shown to reduce the accumulation of body fat.[8] It remains unclear how a lack of myostatin can suppress adipocyte accumulation when there is only minimal myostatin expression in fat tissues.

There are at least three types of adipose tissues. White adipose tissue (WAT) serves as a depot of stored energy, whereas brown adipose tissues (BATs) contain higher numbers of mitochondria. In BAT, an uncoupling protein on the inner membrane of mitochondria functions to uncouple oxidative phosphorylation and hence, is involved in regulating body temperature.[11] Recently, a third type of adipocyte, 'brite' or beige adipocytes in WAT has been characterized as an inducible 'brown-like' adipocyte.[12,13] For example, in mice living at cold temperatures or receiving a β3-adrenergic agonist or exercising, WAT acquires BAT-like properties, with increased brown adipocytes and enhanced expression of uncoupling protein 1 (UCP1).[14–17] A proposed mechanism that increase the 'browning' of WAT would be a rise in peroxisome proliferator-activated receptor gamma, coactivator 1α (PGC-1α) followed by increased expression of *Fndc5* (Fibronectin type III domain-containing protein).[17] The Fndc5 protein contains an N-terminal signal peptide, a fibronectin type III domain and a

[1]College of Life Sciences, Sichuan University, Chengdu, China; [2]Nephrology Division, Department of Medicine, Selzman Institute for Kidney Health, Baylor College of Medicine, Houston, TX, USA and [3]Department of Cardiovascular Biology, Beijing Institutes of Heart, Lung, and Blood Vessel Diseases, An Zhen Hospital Affiliated to Capital Medical University, Beijing, China. Correspondence: Dr L Zhang, Selzman Institute for Kidney Health, Nephrology Division, Department of Medicine, Baylor College of Medicine, One Baylor Plaza, M/S: BCM 395 ABBR R705, Houston 77030 TX, USA or Professor F Chen, College of Life Sciences, Sichuan University, Chengdu 610065, China.
E-mail: lipingz@bcm.edu or chenfang@scu.edu.cn
[4]These authors contributed equally to this work.

transmembrane domain. Removal of the transmembrane domain results in release of the extracellular fragment of the protein and production of a novel molecule, irisin. Irisin reportedly stimulates the differentiation of myoblasts and the browning of WAT in subcutaneous fatty tissue.[17,18] BAT reportedly regulates whole-body energy expenditure, glucose homeostasis and insulin sensitivity.[17,19,20]

The development of a myostatin KO mouse model led to the finding that adipocyte accumulation is decreased while insulin sensitivity is improved even when mice fed with HFD. However, the genetic model does not clarify whether myostatin deficiency directly contributes to the decrease in adipocyte accumulation and insulin sensitivity. We stimulated myostatin production in mice fed a HFD and tested the hypothesis that non-genomic inhibition of myostatin would improve their insulin resistance.

MATERIALS AND METHODS

Reagents
The primary antibodies against p-Akt (Ser473), Akt, p-Smad2, p-Smad3, PPARγ, p-ACC1 and PGC-1α were from Cell Signaling Technology (Beverly, MA, USA). Antibodies against F4/80, CD68, Fndc5 and UCP1 were from Abcam (Cambridge, MA, USA). ELISA kits for measuring irisin, interleukin (IL)-6 or adiponectin were from BioVision (Milpitas, CA, USA), eBioscience (San Diego, CA, USA) or R&D Systems (Minneapolis, MN, USA), respectively. The recombinant proteins, irisin or myostatin were obtained from Enzo life Sciences (Farmingdale, NY, USA) or R&D systems. The anti-myostatin peptibody (peptibody) was from Atara Biotherapeutics (Westlake Village, CA, USA).[21,22] Serum insulin concentration was measured using the Rat/Mouse Insulin ELISA kit (Millipore, Billerica, MA, USA). Serum-free fatty acid levels were measured using the NEFA C kit from Wako (Richmond, VA, USA).

Animals
All experimental procedures were approved by the Institutional Animal Care and Use Committee of Baylor College of Medicine. C57BL/6 mice were purchased from Jackson Laboratory (Bar Harbor, ME, USA).

At 6 weeks of age, 40 male mice with comparable body weights were divided into four groups of 10 mice. We estimated that $n = 10$ mice would be needed to achieve an alpha of 0.01 and a power of 80% based on a mean body weight change of 8% and standard deviation of ± 5%. Two groups were fed the HFD (58% kcal from fat, Research Diets, New Brunswick, NJ, USA). The other groups were fed the regular diet (RD: 11% kcal from fat). After 12 weeks of the HFD, 10 mice from the control group and 10 mice fed the HFD were given intraperitoneal (i.p.) injections of 5 mg kg^{-1} of the anti-myostatin peptibody (murine Fc fusion PINTA 745/Mu-S) every other day for 4 weeks; control mice were fed the RD or HFD and injected every other day i.p. with same volume of phosphate-buffered saline (PBS) as described.[6] The same diet was fed to mice throughout the 16 weeks. Previously, we documented that the peptibody blocked myostatin activity measured as suppression of p-Smad2/3 activity and the promoter activity of Smad2/3.[6] The peptibody specifically suppress myostatin activity but do not suppress activin A. It exhibited an IC50 for inhibition of myostatin activity at 1.2 nM. Administration of the peptibody into mice with chronic kidney disease increased their muscle and body weight.[6]

Body weights and food intake were measured daily. Before and 4 weeks after beginning peptibody injections, lean and fat mass of individual mice were quantified using an X-ray Imager (PIXImus Body Composition, Lunar Corp, Madison, WI, USA). At the end of the experimental period, oxygen consumption (V_{O2}) and carbon dioxide production (V_{CO2}) were measured using a comprehensive laboratory animal monitoring system equipped with an Oxymax Open Circuit Calorimeter (Columbus Instruments, Columbus, OH, USA). The volumes of oxygen (V_{O2}) and the volume of carbon dioxide (V_{CO2}) were used to calculate the respiratory exchange ratio (RER = V_{CO2}/V_{O2}). At the time the mice were killed, gastrocnemius, tibialis anterior, soleus and extensor digitorum longus muscles plus interscapular BAT and abdominal adipose tissues (subcutaneous and visceral adipose tissues) were dissected, weighed and immediately frozen in liquid nitrogen. The samples were stored at − 80 °C.

At the beginning and end of treatments with peptibody injections, mice were fasted for 16 h and a glucose tolerance test was measured: fasted mice were injected i.p. with 2 mg kg^{-1} glucose and tail vein blood was collected at 0, 30, 60 and 120 min intervals to assess blood glucose concentration using a True Track Glucometer (Nipro Diagnostics, Fort Lauderdale, FL, USA). On another day, an insulin tolerance test was performed in mice fasted for 4 h: mice were injected i.p. with 2 U kg^{-1} insulin and blood was collected after 0, 30, 60 and 120 min to measure blood glucose concentration. Changes in blood glucose were analyzed as the area under curve method using Statstodo program (http://www.statstodo.com/AUC_Exp.php).

Isolation and differentiation of stem cells derived from adipose tissue
Visceral adipose tissue was minced into 2–5 mm^2 pieces followed by digestion with 1.5 mg ml^{-1} collagenase II at 37 °C for 2 h. After stopping the reaction with Dulbecco's modified Eagle's medium containing 10% fetal bovine serum, the mixture was filtered (100 μM) before centrifugation at 450 g for 5 min. Cells in the pellet were suspended in Dulbecco's modified Eagle's medium containing 20% fetal bovine serum and 1% penicillin/streptomycin. Adipose cells were cultured at 37 °C in 5% CO$_2$ for 3 days, followed by changing to fresh medium every 2 days. At confluence, cells were subjected to adipogenic differentiation by culturing in Dulbecco's modified Eagle's medium supplemented with 20% fetal bovine serum and 11.5 μg ml^{-1} isobutylmethylxanthine, 1 μg ml^{-1} insulin plus 1 μM dexamethasone; differentiated cells were incubated with 20 nM irisin for 2 days.

Myostatin knockdown in C2C12 cells
Mouse C2C12 myoblasts (American Type Culture Collection, Manassas, VA, USA) were transduced with lentivirus expressing small hairpin RNA (ShRNA)-myostatin or ShRNA-control (Santa Cruz Technology, Dallas, TX, USA) as described before.[21] In brief, C2C12 cells were plated into 12 wells, 24 h later, C2C12 cells at 50% confluence were transduced with 20 μl of 1 × 10^6 infectious units of virus of ShRNA-myostatin or ShRNA-control plus 8 μg ml^{-1} polybrane. We measured irisin expression and production in these cells.

RNA extraction and quantitative real-time PCR
RNA was isolated from gastrocnemius muscles or adipose tissue using RNeasy kit (Qiagen, Valencia, CA, USA). As described, we performed RT-PCR to obtain relative gene expression by calculating the cycle threshold (Ct) values using glyceraldehyde 3-phosphate dehydrogenase (GAPDH) as an internal control (relative expression = $2^{(sample\,Ct - GAPDH\,Ct)}$).[23] Primers sequences will be provided upon request.

Immunohistochemical staining
Cryo-sections (10 μM) of the midbelly region of tibialis anterior muscles were fixed in 4% paraformaldehyde and incubated with anti-CD68 before exposing them to an Alexa Fluor-conjugated secondary antibody (Invitrogen, Grand Island, NY, USA). Paraffin sections (5 μM) of adipose tissue were immunostained with anti-UCP1 or F4/80. The antibodies were incubated with the sample for 1 h at room temperature followed by incubation for 30 min with biotinylated antibodies. UCP1- or F4/80-positive cells in five randomly chosen areas were counted by an observer blinded to peptibody vs PBS treatments. The results were expressed as the percentage of adipose cell nuclei that were positive for UCP1 or F4/80.

Muscle triglycerides
The triglyceride level in the muscle was measured by the PicoProbe Triglyceride Quantification Assay Kit (Abcam). Briefly, 20 mg gastrocnemius muscle was homogenized with 200 μl ice-cold Triglyceride Assay Buffer. The supernatant after centrifugation (16 000 r.p.m. 10 min at 4 °C) was collected and 50 μl were used to measure triglycerides by fluorescence (Ex/Em = 535/587 nm) in a microplate reader.

Isolation of mouse peritoneal macrophages
Mice were injected intraperitoneally with 2 ml of 3% thioglycollate. After 4 days, peritoneal cells were collected as described.[24] Cells were stimulated by 10 μg ml^{-1} lipopolysaccharides, 20 nM irisin or 100 ng ml^{-1} myostatin.

Statistical analysis

Results are expressed as means ± s.e.m. Significance testing was performed using one-way analysis of variance followed by pair-wise comparisons using the Student–Newman–Keuls test. Statistical significance was set at $P < 0.05$. A minimum of three replicates were performed for each experimental condition.

RESULTS

Myostatin inhibition stimulates muscle growth

C57BL/6 mice fed a HFD for 16 weeks were compared with mice fed the RD. The HFD led to a significant increase in glucocorticoid
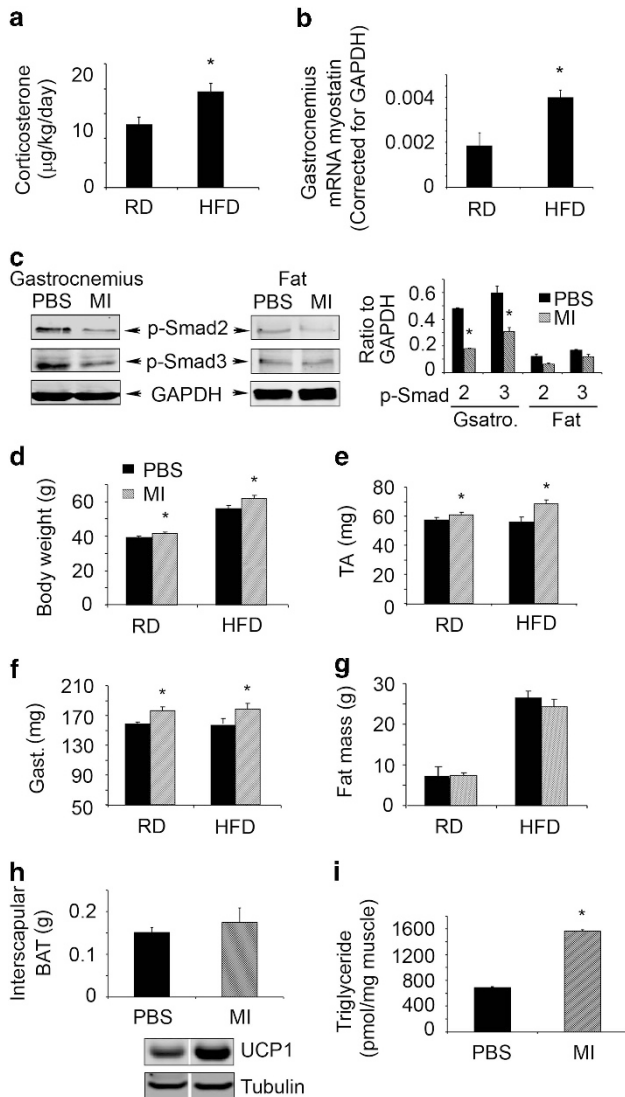
Figure 1. Myostatin inhibition stimulates muscle growth despite feeding a HFD. (**a**) Twelve weeks after HFD-fed mice, glucocorticoid production was estimated as the daily excretion of corticosterone. (**b**) Twelve weeks after HFD-fed mice, myostatin mRNA was measured in gastrocnemius muscles. (**c**) Four weeks after HFD-fed mice treated with PBS or peptibody, p-Smad2/3 was evaluated by western blots in gastrocnemious muscle and visceral fat tissue. (**d**–**i**) Four weeks after HFD-fed mice treated with PBS or peptibody: (**d**) body weights; (**e**) tibialis anterior (TA) muscle weights; (**f**) gastrocnemius (Gast.) muscle weights; (**g**) fat mass; (**h**) interscapular brown adipocyte weights and (**i**) triglyceride level in muscle (results are mean ± s.e.m.; *$P < 0.05$ vs control RD or HFD mice treated with PBS. $n = 10$ mice in each group. MI, myostatin inhibition).

production (Figure 1a) and increased myostatin mRNA in muscles (Figure 1b).[21] Next, we evaluated the consequences of blocking myostatin by injecting mice fed the HFD with the peptibody every other day for 4 weeks and compared results to those in mice fed the HFD but injected with PBS. After 4 weeks of peptibody treatment of the HFD mice, there was a significant decrease in p-Smad2/3 in muscles vs results in HFD mice treated with PBS. There also were low levels of p-Smad2/3 in visceral adipocytes (Figure 1c). These results suggest that the peptibody effectively blocked myostatin activity in muscle and potentially in adipose tissues.[6;25] Blocking myostatin significantly increased the weights of body (Figure 1d) and muscle (Figures 1e and f), even though the intake of food was not different. We also measured intra-abdominal adipose tissue using the X-ray Imager and found that myostatin inhibition slightly but not significantly decreased the mass of adipose tissue (Figure 1g). Peptibody treatment slightly increased the mass and activity of interscapular BAT (Figure 1h); there also was an increase in muscle triglycerides in peptibody-treated mice fed the HFD compared with results in control mice treated with PBS (Figure 1i). Thus, myostatin inhibition in mice increases muscle growth despite feeding a HFD.

Myostatin inhibition suppresses macrophage infiltration and inflammatory gene expression in muscle and adipose tissues

To examine whether myostatin inhibition reduces the expression of proinflammatory cytokines in muscle or adipose tissues, we fed the HFD to mice for 12 weeks and then treated them with the peptibody or PBS for 4 weeks.[9] In muscles of mice fed the HFD and treated with the peptibody, exhibited a significant decrease in the mRNAs of IL-6, tumor necrosis factor (TNF)-α and monocyte chemotactic protein 1 (MCP1) (Figure 2a). The mechanism for the decrease in inflammatory cytokine expression might be related to suppressed macrophage infiltration into muscles.[26] To test this hypothesis, we immunostained muscle sections from mice fed the HFD and found higher levels of the macrophage marker, CD68, and myostatin inhibition suppressed it (Figure 2b). These results were confirmed when we evaluated the expression of mRNAs encoding the macrophage markers, CD68 and F4/80 (Figure 2c).

Similar results were found in subcutaneous and visceral adipose tissues of mice that had been treated with the peptibody (Figures 2d and e). The number of macrophages infiltrating adipose tissues was suppressed by the inhibition of myostatin. Likewise, in visceral adipose tissues of mice fed the HFD and treated with the peptibody, we found the mRNAs of cytokines and chemokines (TNF-α, IL-6, MCP1, macrophage inflammatory protein-1β and so on) were significantly suppressed (Figure 2f). Thus, inhibiting myostatin suppressed HFD-induced infiltration of macrophages and the expression of inflammatory genes in both muscle and adipose tissues.

Previously, we found that recombinant myostatin stimulated IL-6 production in muscle cells.[6] To explore whether myostatin stimulates inflammatory signaling in adipocytes or immune cells, we isolated pre-adipocyte cells from visceral adipose tissues of HFD mice. The cells were differentiated into adipocyte with adipocyte differentiation media and then treated with recombinant myostatin. Within 5 h, there was an increase in IL-6 in the medium of cells treated with recombinant myostatin (Figure 2g). We also isolated mouse peritoneal macrophages and treated them with recombinant myostatin. There was an increased IL-6 production from 16 to 48 h (Figure 2h). These results indicate that myostatin stimulates inflammatory signaling pathways in skeletal muscle, adipocytes and in macrophages.

Myostatin inhibition improves insulin sensitivity in mice fed the HFD

We measured glucose tolerance test and insulin tolerance test in HFD-fed mice that had been treated with the peptibody or PBS. The results were compared with those of mice fed with RD and treated
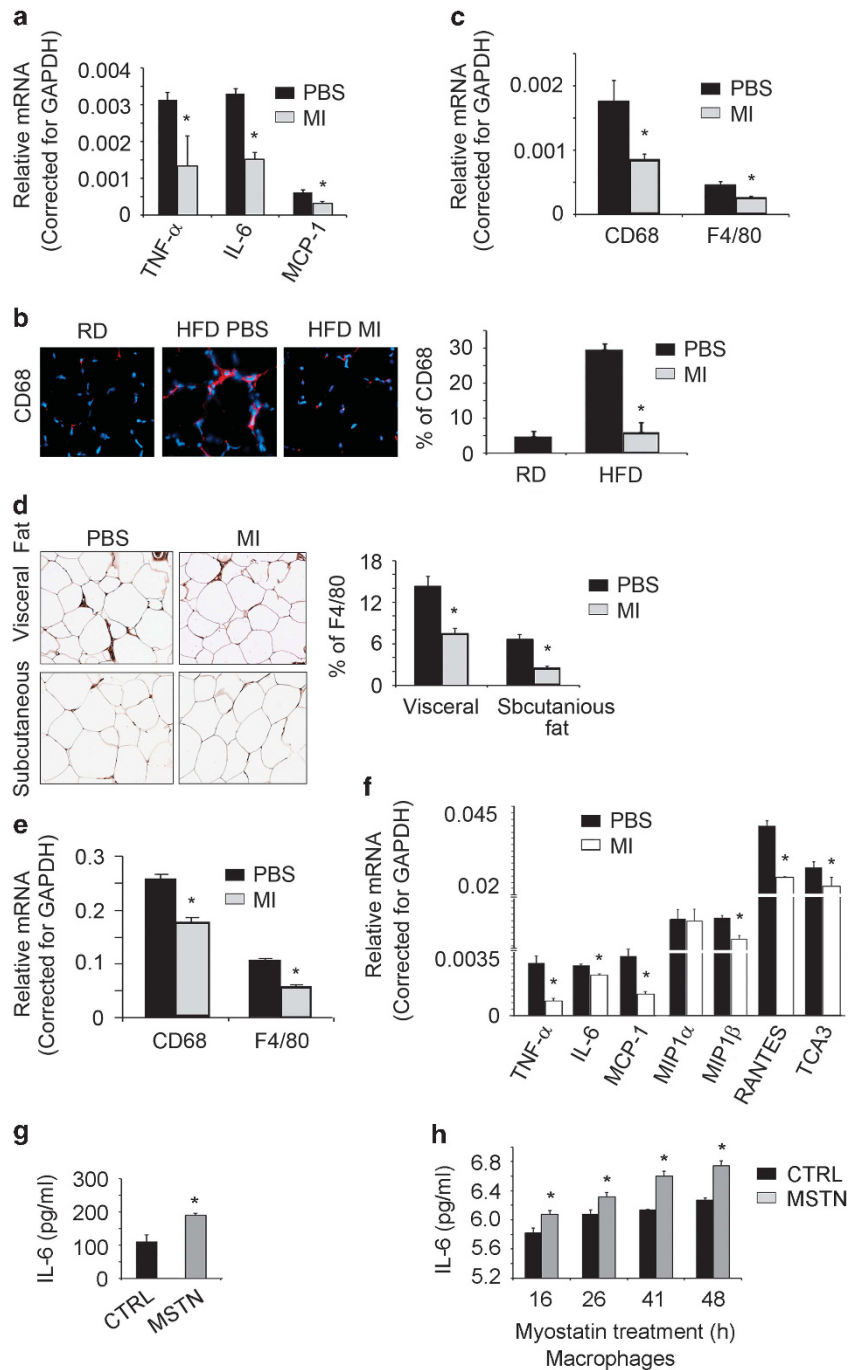
Figure 2. Myostatin inhibition suppresses macrophage infiltration and inflammatory gene expression in skeletal muscle and adipose tissues. Mice were treated as described in the Figure 1 and the following measurements were obtained. (a) IL-6, TNF-α and MCP1 mRNA in gastrocnemius muscles (corrected for GAPDH); (b) cross-sections of tibialis anterior muscles that were immunostained with anti-CD68 (red, left panel). The percentage of muscle nuclei that stained positive for CD68 was determined in five randomly chosen areas (right panel). (c) Macrophage-specific mRNAs in gastrocnemius muscles. (d) Cross-sections of subcutaneous or visceral adipose tissue were immunostained with anti-F4/80. The percentage of adipose cell nuclei that stained positive for F4/80 was determined in five randomly chosen areas (right panel). (e) Macrophage-specific mRNAs in visceral adipose tissues. (f) The mRNAs of cytokines or chemokines in visceral adipose tissue. (g) Myostatin stimulate IL-6 production in adipocyte within 5 h. (h) Myostatin stimulate IL-6 production in macrophages from 16 to 48 h (results are mean ± s.e.m.; *P < 0.05 vs PBS or control (CTRL). n = 3 mice in each group or cell treatment repeated in three times. MI, myostatin inhibition; MSTN, myostatin treatment).

with the peptibody or PBS. In mice fed the control diet, myostatin inhibition did not change blood glucose concentration but in mice fed the HFD and treated with the peptibody, fasting levels of glucose and insulin were decreased compared HFD-fed mice treated with PBS (Figures 3a and b; P < 0.05). Glucose tolerance test

and insulin tolerance test measurements confirmed that myostatin inhibition significantly improved glucose metabolism (Figures 3c and d). We also found that inhibiting myostatin reduced circulating free fatty acids and increased the blood level of adiponectin (Figures 3e and f). These changes are consistent with reports that
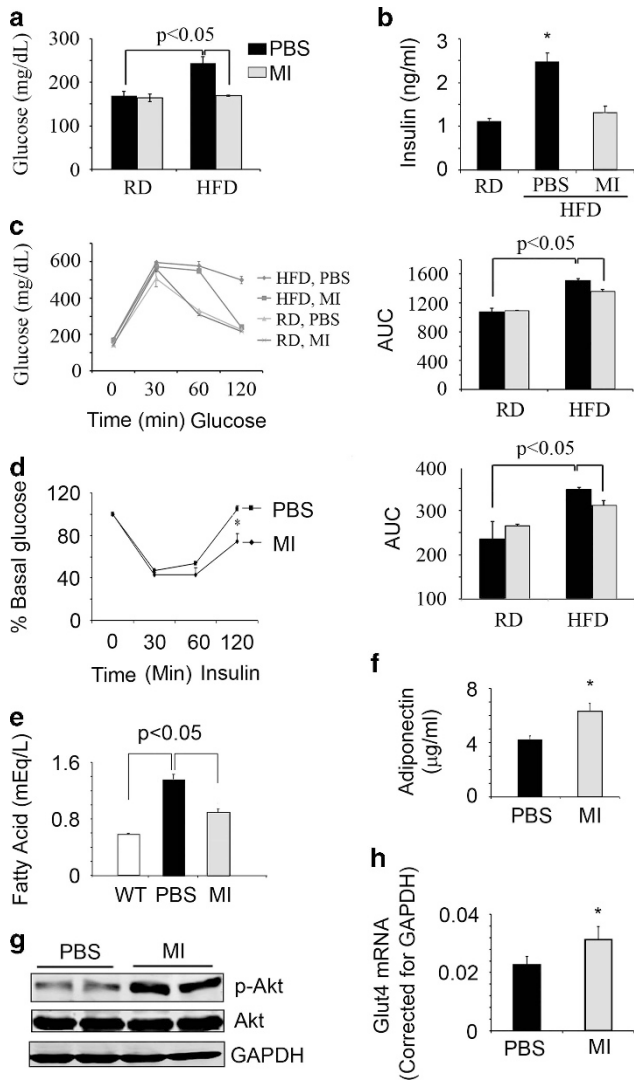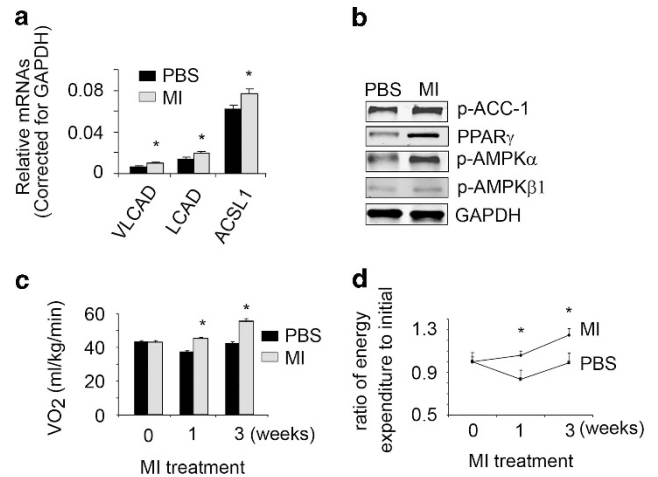
Figure 3. Myostatin inhibition increases insulin sensitivity in mice despite the HFD. Mice were treated as described in the Figure 1 legend. (a, b) After 4 weeks of treatment with the peptibody, fasting blood glucose and serum insulin levels were measured. (c) Results of a glucose tolerance test (left panel) and calculated area under curve (AUC; right panel) are presented. (d) Results of the insulin tolerance test (left panel) and calculated AUC (right panel) are presented. (e) Levels of serum fatty acids and (f) adiponectin are presented. (g) p-Akt in gastrocnemius muscles of mice are shown. (h) Glut4 mRNA in gastrocnemius muscles of mice. (results are mean ± s.e.m.; *$P < 0.05$ vs PBS. $n = 10$ mice in each group. MI, myostatin inhibitor).

adiponectin improves insulin sensitivity by inhibiting hepatic gluconeogenesis and increasing fatty acid oxidation in the liver and the muscle.[27-29] Mice fed the HFD and treated with the peptibody had higher levels of p-Akt in muscles compared with values in HFD-fed mice treated with PBS (Figure 3g). Improved insulin signaling in muscle was confirmed by finding an increase in the mRNA of the muscle glucose transporter, Glut4 (Figure 3h). We conclude that the peptibody improves insulin signaling in mice despite the insulin resistance stimulated by the HFD.

Myostatin inhibition increases fatty acid oxidation and energy expenditure

To examine whether myostatin inhibition improves fatty acid metabolism, we assessed the mRNAs of genes involved in fatty acid
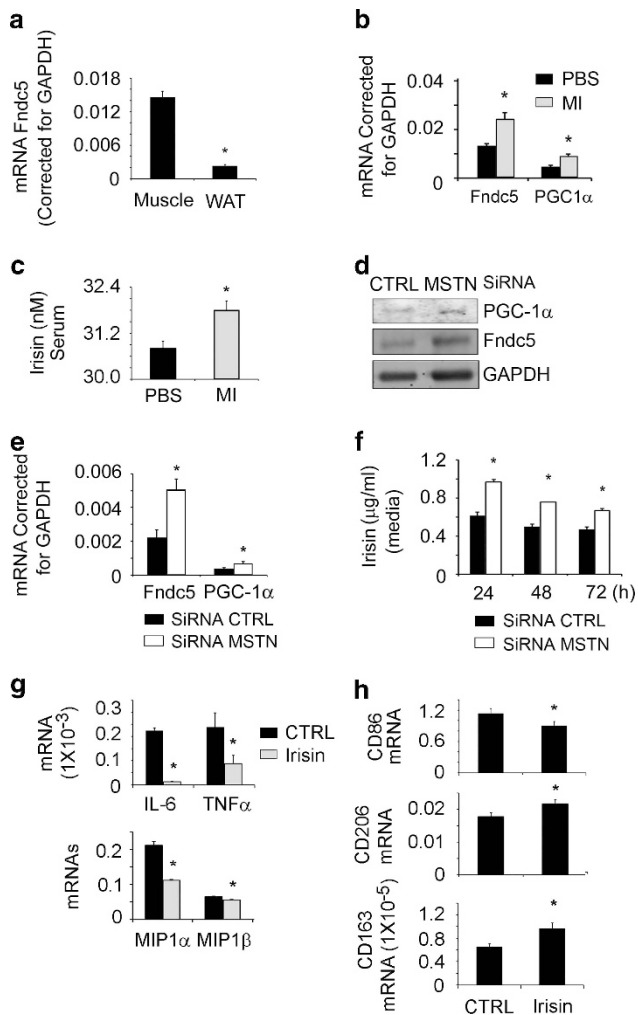

Figure 4. Myostatin inhibition increases fatty acid oxidation and energy expenditure. (a) In gastrocnemius muscles of mice fed the HFD and treated with the peptibody or PBS, there were higher mRNAs of enzymes involved in fatty acid oxidation (long-chain acyl-CoA dehydrogenase (LCAD); very long-chain acyl-CoA dehydrogenase (VLCAD) and acyl-CoA synthetase long-chain family member 1 (ACSL1)). (b) In gastrocnemious muscles, proteins involved in mitochondrial function was evaluated by western blot analysis. (c, d) Changes in oxygen consumption (V_{O_2}) and energy expenditure over 3 weeks were calculated from values measured before mice received the peptibody (results are mean ± s.e.m.; *$P < 0.05$ vs PBS. $n = 10$ mice in each group. MI, myostatin inhibitor).

oxidation: long-chain acyl-CoA dehydrogenase; acyl-CoA synthetase long-chain family member 1 and very long-chain acyl-CoA dehydrogenase. Each was upregulated in muscles (Figure 4a) and in WAT (results not shown). Treatment of HFD-fed mice with the peptibody increased phospho-acetyl-CoA carboxylase (p-ACC), phospho-adenosine 5'-monophosphate-activated protein kinase α (p-AMPK) and peroxisome proliferator-activated receptor γ (PPARγ) in muscles (Figure 4b), consistent with the conclusion that inhibition of myostatin stimulates fatty acid oxidation. In fact, circulating fatty acids in mice fed the HFD were substantially reduced by the peptibody (Figure 3e). Energy expenditure in HFD mice treated with the peptibody included an increase in oxygen consumption and the respiratory exchange ratio (Figures 4c and d) suggesting that myostatin inhibition not only stimulates fatty acid oxidation in muscle but also increases energy expenditure.

Myostatin inhibition increases irisin expression

As exercise improves insulin resistance and increases irisin production, we examined whether irisin has a role in the responses of myostatin inhibition and the improvement of insulin sensitivity. In normal mice, the irisin precursor protein, Fndc5, is highly expressed in the muscle but minimally in WAT (Figure 5a). Following 4 weeks of peptibody treatment of HFD mice, Fndc5 mRNA in muscle was significantly higher vs results in muscles of PBS-treated mice fed the HFD. In addition, the mRNA of PGC-1α, an upstream activator of Fndc5 was increased (Figure 5b). We also found that irisin is increased in the serum of mice treated with the peptibody (Figure 5c).

To examine how myostatin inhibition influences Fndc5 expression and irisin production in the muscle, we examined cultured C2C12 muscle cells. First, we knocked down myostatin in these cells using ShRNA.[21] In cells lacking myostatin, the Fndc5 protein and its upstream activator, PGC-1α, were increased (Figure 5d). Knocking down myostatin also increased the expression of mRNAs encoding Fndc5 and PGC-1α (Figure 5e). Finally, at 24–72 h after knocking down myostatin in C2C12 cells, we found increased irisin

Figure 5. Myostatin inhibition increases Fndc5 expression in muscles of mice fed the HFD. (**a**) mRNA values (corrected for GAPDH) are shown for Fndc5 in the muscle and in subcutaneous white adipose tissue. (**b**) Relative Fndc5 mRNA expression in skeletal muscles of mice fed the HFD and treated with the peptibody. (**c**) Treatment with the peptibody increased serum irisin levels compared with values in mice treated with PBS. (**d, e**) When myostatin production was blocked in C2C12 cells, the protein (**d**) and mRNA (**e**) expressions of PGC-1α and Fndc5 are increased. (**f**) Suppression of myostatin raised the production of irisin in C2C12 cells. (**g**) Irisin inhibit cytokine and chemikine mRNA expression in macrophages. (**h**) Irisin stimulates macrophage polarization from M1 to M2 (results are mean ± s.e.m.; *$P < 0.05$ vs control (CTRL). MI, myostatin inhibition; MSTN, myostatin treatment).

production (Figure 5f). Thus, myostatin inhibition increases the expression and metabolic functions of Fndc5 in muscle cells.

To examine if irisin exerts anti-inflammatory functions, we activated peritoneal macrophages with lipopolysaccharides and then added recombinant irisin. The addition of irisin decreased the expression of inflammatory markers (Figure 5g) and stimulated macrophage polarization from M1 into M2 by decreasing the mRNA expression of CD86 (M1 marker) while increasing the mRNA expression of CD163 and CD206 (M2 marker; Figure 5h).

Myostatin inhibition stimulates browning of WAT by an irisin-mediated mechanism

In WAT from mice fed the HFD and treated with the peptibody, BAT mRNA markers including Cidea, PRDM16, UCP1 and PGC-1α were increased (Figure 6a). Similarly, mRNA markers of beige

adipocytes, Tbx1 and Tmem26, were higher (Figure 6a).[13] In consistent with mRNA expression, we immunostained the cross-section of subcutaneous or visceral adipose tissue with anti-UCP1 and found myostatin inhibition increased UCP1 expression in WAT (Figure 6b). These results lead us to conclude that inhibition of myostatin stimulates 'browning' of WAT.

To explore whether irisin is responsible for inducing the browning of WAT, we isolated stem cells from visceral adipocytes. When they were confluent, we treated them with recombinant irisin for 3 days and found increased UCP1 and PGC-1α proteins (Figure 6c). Notably, when we treated adipocyte-derived stem cells with conditioned media from C2C12 cells lacking myostatin, there were increases in the markers of beige and BAT marker mRNAs, PRDM16, PGC-1α, UCP1 and Cidea (Figure 6d).

To prove that conditioned medium from C2C12 cells lacking myostatin contains irisin capable of inducing adipose-derived stem cells to express markers of brown adipocytes, we added an anti-Fndc5 antibody to adipocyte-derived stem cells before adding conditioned medium. The anti-Fndc5 antibody abolished the expression of genes involved in browning of adipocyte-derived stem cells (Figure 6e). These results uncover a cross talk by which irisin produced in muscle cells promotes browning of WAT.

DISCUSSION

Obesity is associated with the increased accumulation of fatty tissue and a relative decrease in lean and muscle mass.[30] In obese individuals, adipose tissue has been linked to insulin resistance and type 2 diabetes developing via proinflammatory cytokines.[31] Not only is muscle an important site of fatty acid oxidation but also skeletal muscle is responsible for >75% of insulin-mediated glucose metabolism.[31,32] The latter suggests that reduced muscle mass develops in response to insulin resistance and it is established that chronic inflammation and oxidative stress contribute to skeletal muscle insulin resistance.[31] In the present study, we have found that myostatin expression and secretion are increased in mice with HFD-induced obesity, potentially linking myostatin to the development of insulin resistance. Indeed, administration of the peptibody to HFD-fed mice increased muscle growth and suppressed macrophage infiltration and proinflammatory gene expression in skeletal muscle and adipose tissues. Inhibition of myostatin also improved glucose homeostasis, energy expenditure and increased the browning of WAT. Finally, we found that a mediator of myostatin-induced responses is irisin: myostatin inhibition upregulates the expression of irisin in the muscle and serum and induces browning of WAT with improved insulin sensitivity of HFD-fed mice. Thus, our results reveal a cross talk between skeletal muscle and WAT via myostatin and irisin regulation, suggesting that regulation myostatin represents a promising therapeutic target to treat obesity and potentially, type 2 diabetes.

How does myostatin affect insulin resistance? First, conditions associated with a high myostatin level often exhibit evidence of inflammation. For example, Wilkes et al. fed a HFD to control and myostatin KO mice and found that the control mice but not those lacking myostatin developed insulin resistance.[9] The authors suggested that these changes were related to a myostatin-stimulated expression of TNF-α, an established mediator of insulin resistance.[9] Likewise, we have found that chronic kidney disease, a condition often associated with insulin resistance induces expression of myostatin, IL-6 and TNF-α in the muscle.[6] Inhibition of myostatin suppressed IL-6 and TNF-α production in muscle. Currently, we showed that blocking myostatin in HFD-fed mice not only suppresses inflammation but also improves insulin resistance (Figures 2 and 3). A second mechanism by which myostatin affects insulin resistance is that myostatin-stimulated phosphorylation of Smad2 and Smad3 transcription factors, they can interact with p-Akt to impair IGF-1 and insulin signaling in the
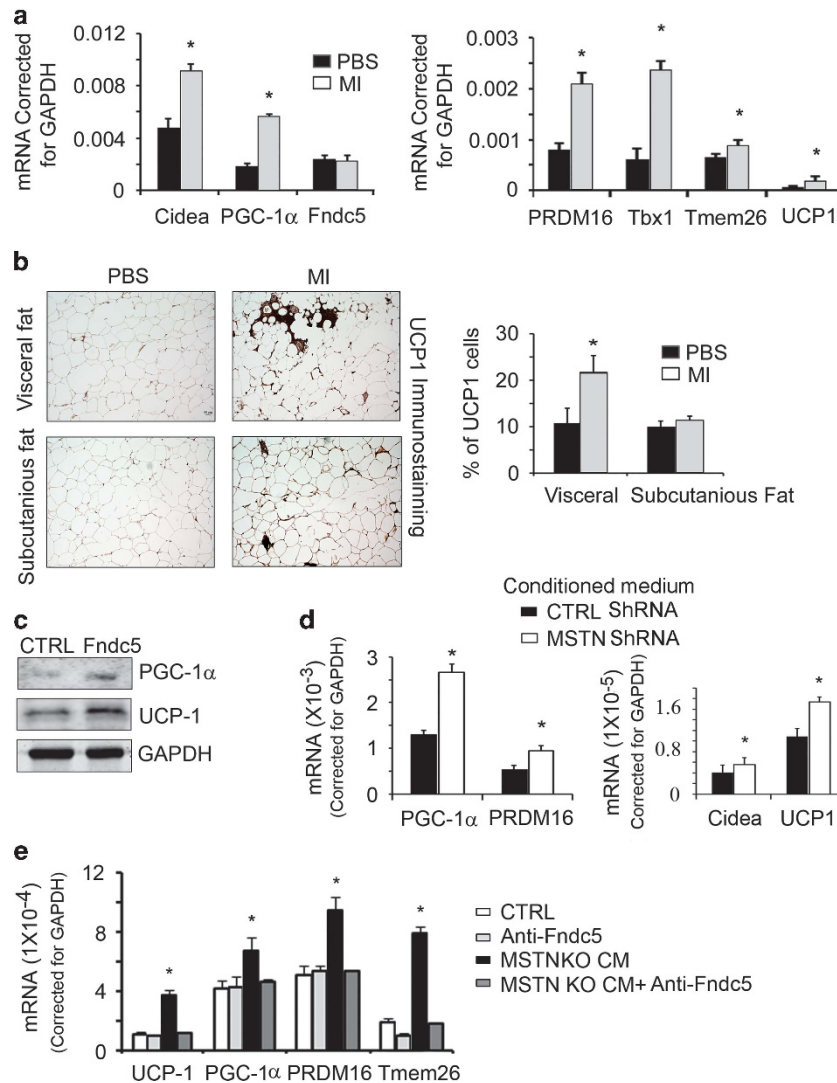
Figure 6. Irisin is a key mediator that induces browning of WAT. (**a**) mRNAs of BAT and beige genes in visceral fat tissue. (**b**) Visceral and subcutaneous adipose tissues were immunostained for UCP1 (brown colour). The percentage of UCP1-positive cells to the number of fat cells examined is shown in the right panel. (**c**) Adipocyte-derived stem cells were treated with 20 nM recombinant irisin. This raised the expression of PGC-1α and UCP1. (**d**) Conditioned media from C2C12 cultured muscle cells lacking myostatin, stimulated the mRNAs of expression of BAT genes in adipocyte-derived stem cells. (**e**) When the C2C12-conditioned medium was treated with a neutralizing antibody to Fndc5, the mRNAs of BAT genes were suppressed (results are mean ± s.e.m.; *$P < 0.05$ vs PBS or control. MI, myostatin inhibition; MSTN, myostatin treatment).

muscle.[33,34] Third, excess triglyceride in the muscle is often associated with insulin resistance.[35] Surprisingly, inhibition of myostatin in mice fed the HFD resulted in increased muscle triglyceride content and improved insulin sensitivity (Figures 1i and 3d). This result is consistent with reports that exercise training increases muscle triglyceride content [36] and chronic exercise increases insulin sensitivity[37] and fatty acid oxidation.[38]

Although myostatin primarily affects muscle growth, we found it also influences whole-body metabolism. For example, we found that blocking myostatin activity increased body weight despite a higher energy expenditure (Figure 1d). This occurred because peptibody-treated mice experienced a significant increase in muscle weight (Figures 1e and f) but only a slight decrease in adipose tissue mass (Figure 1h). The increase in body weight occurring despite a rise in energy expenditure is consistent with previous reports. Akpan et al. reported that myostatin inhibition achieved by injecting HFD-fed mice with a soluble ACVR2B/Fc fusion protein resulted in a greater lean mass but no change in adipose tissue.[39] Bernardo et al. treated ob/ob mice with a

neutralizing monoclonal antibody to myostatin and found that the mice developed increases in activity, oxygen consumption and energy expenditure but no reduction in fat mass.[40] We found that inhibition of myostatin in mice fed the HFD led to browning of subcutaneous and visceral adipocytes plus increased levels of BAT-associated mRNAs, including UCP1, PGC-1α and Cidea in WAT (Figures 5 and 6). The browning response was unexpected because the expression of myostatin in adipocytes is so low that its inhibition would be expected to influence adipose tissue metabolism minimally. Notably, our results are consistent with events occurring in myostatin KO mice: feeding the HFD to those mice did not induce obesity or insulin resistance.[41]

How does myostatin inhibition affect whole-body metabolism? A possible mechanism is that myostatin inhibition induces irisin production in the muscle. This is relevant because irisin has an important role in stimulating UCP1 expression and the browning of WAT.[13,17,42] There is evidence that the browning of WAT increases insulin sensitivity. For example, Stanford et al. transplanted BAT tissue from male, donor mice into age- and
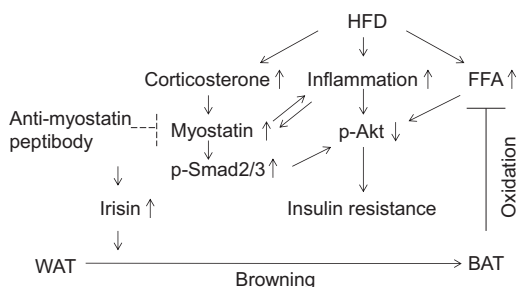
Figure 7. The mechanism of myostatin inhibition leading to improved insulin resistance in mice fed the HFD. Myostatin inhibition suppresses inflammation, increases irisin production, increases fatty acid oxidation and the browning of WAT to reduces free fatty acid (FFA) while improves insulin sensitivity in mice fed the HFD.

gender-matched mice and found that glucose tolerance improved and fat mass was reduced despite being fed a HFD.[43] A similar response occurs in humans when BAT is stimulated: BAT-positive men exposed to cold temperature for 5–8 h increased in resting energy expenditure and whole-body glucose disposal and insulin sensitivity.[44]

How does the inhibition of myostatin stimulate irisin production in the muscle? We speculate that the mechanism is related to PGC-1α expression in the muscle because myostatin inhibition in HFD-fed mice leads to increases in the mRNAs of PGC-1α and Fndc5 (Figure 5b). In C2C12 muscle cells, knockdown of myostatin stimulates the expression of the mRNAs and proteins of PGC-1α and Fndc5 (Figures 5d and e). Consistent with these results, exercise can increase the mRNAs and proteins of PGC-1α in skeletal muscles.[17,45,46] It also has been shown that PGC-1α expression is increased in muscles of myostatin KO mice.[47] This is important because PGC-1α is an upstream activator of Fndc5. In addition, AMPK-α is activated in muscles of myostatin KO mice.[47,48] Consistent with these reports, we found that myostatin inhibition in HFD-fed mice stimulated phosphorylation of AMPK-α (Figure 4). This is relevant because myostatin KO causes a switch in muscle fibers to raise the fast myosin heavy-chain isoform.[49–51] This myofiber contracts faster and utilizes glycolytic metabolic pathways with an increase in AMP/ATP, leading to more robust activation of AMPK.[52] AMPK is functioning as activator of PGC-1α.[48] Therefore, inhibition myostatin in HFD mice activate AMPK to stimulate PGC-1α and Fndc5 expression to mediate the browning of WAT.[48]

In summary, our present study elucidates that inhibition myostatin leads to improved insulin resistance in mice fed the HFD. We have demonstrated that myostatin inhibition suppresses inflammation, increases fatty acid oxidation and the browning of WAT while improving insulin sensitivity in mice fed the HFD (Figure 7). These results enhance our understanding of the function of myostatin and they provide information that myostatin signaling represents a promising therapeutic target for the treatment of obesity and, potentially, diabetes.[53–58]

CONFLICT OF INTEREST

The authors declare no conflict of interest.

AUTHOR CONTRIBUTIONS

JD, YD and LZ conceived and designed the experiments; JD, YD, YLD and LZ performed the experiments; JD, YD, LZ analyzed the data; WEM, CF and LZ wrote the paper.

REFERENCES

1 McPherron AC, Lawler AM, Lee SJ. Regulation of skeletal muscle mass in mice by a new TGF-beta superfamily member. *Nature* 1997; **387**: 83–90.
2 McPherron AC, Lee SJ. Double muscling in cattle due to mutations in the myostatin gene. *Proc Natl Acad Sci USA* 1997; **94**: 12457–12461.
3 Kambadur R, Sharma M, Smith TP, Bass JJ. Mutations in myostatin (GDF8) in double-muscled Belgian Blue and Piedmontese cattle. *Genome Res* 1997; **7**: 910–916.
4 Clop A, Marcq F, Takeda H, Pirottin D, Tordoir X, Bibe B et al. A mutation creating a potential illegitimate microRNA target site in the myostatin gene affects muscularity in sheep. *Nat Genet* 2006; **38**: 813–818.
5 Schuelke M, Wagner KR, Stolz LE, Hubner C, Riebel T, Komen W et al. Myostatin mutation associated with gross muscle hypertrophy in a child. *N Engl J Med* 2004; **350**: 2682–2688.
6 Zhang L, Rajan V, Lin E, Hu Z, Han HQ, Zhou X et al. Pharmacological inhibition of myostatin suppresses systemic inflammation and muscle atrophy in mice with chronic kidney disease. *FASEB J* 2011; **25**: 1653–1663.
7 Lin J, Arnold HB, la-Fera MA, Azain MJ, Hartzell DL, Baile CA. Myostatin knockout in mice increases myogenesis and decreases adipogenesis. *Biochem Biophys Res Commun* 2002; **291**: 701–706.
8 McPherron AC, Lee SJ. Suppression of body fat accumulation in myostatin-deficient mice. *J Clin Invest* 2002; **109**: 595–601.
9 Wilkes JJ, Lloyd DJ, Gekakis N. Loss-of-function mutation in myostatin reduces tumor necrosis factor alpha production and protects liver against obesity-induced insulin resistance. *Diabetes* 2009; **58**: 1133–1143.
10 Guo T, Jou W, Chanturiya T, Portas J, Gavrilova O, McPherron AC. Myostatin inhibition in muscle, but not adipose tissue, decreases fat mass and improves insulin sensitivity. *PLoS One* 2009; **4**: e4937.
11 Cannon B, Nedergaard J. Brown adipose tissue: function and physiological significance. *Physiol Rev* 2004; **84**: 277–359.
12 Walden TB, Hansen IR, Timmons JA, Cannon B, Nedergaard J. Recruited vs. nonrecruited molecular signatures of brown, "brite," and white adipose tissues. *Am J Physiol Endocrinol Metab* 2012; **302**: E19–E31.
13 Wu J, Bostrom P, Sparks LM, Ye L, Choi JH, Giang AH et al. Beige adipocytes are a distinct type of thermogenic fat cell in mouse and human. *Cell* 2012; **150**: 366–376.
14 Guerra C, Koza RA, Yamashita H, Walsh K, Kozak LP. Emergence of brown adipocytes in white fat in mice is under genetic control. Effects on body weight and adiposity. *J Clin Invest* 1998; **102**: 412–420.
15 Guerra C, Koza RA, Walsh K, Kurtz DM, Wood PA, Kozak LP. Abnormal non-shivering thermogenesis in mice with inherited defects of fatty acid oxidation. *J Clin Invest* 1998; **102**: 1724–1731.
16 Vegiopoulos A, Muller-Decker K, Strzoda D, Schmitt I, Chichelnitskiy E, Ostertag A et al. Cyclooxygenase-2 controls energy homeostasis in mice by de novo recruitment of brown adipocytes. *Science* 2010; **328**: 1158–1161.
17 Bostrom P, Wu J, Jedrychowski MP, Korde A, Ye L, Lo JC et al. A PGC1-alpha-dependent myokine that drives brown-fat-like development of white fat and thermogenesis. *Nature* 2012; **481**: 463–468.
18 Ferrer-Martinez A, Ruiz-Lozano P, Chien KR. Mouse PeP: a novel peroxisomal protein linked to myoblast differentiation and development. *Dev Dyn* 2002; **224**: 154–167.
19 Stanford KI, Goodyear LJ. The therapeutic potential of brown adipose tissue. *Hepatobiliary Surg Nutr* 2013; **2**: 286–287.
20 Harms M, Seale P. Brown and beige fat: development, function and therapeutic potential. *Nat Med* 2013; **19**: 1252–1263.
21 Dong Y, Pan JS, Zhang L. Myostatin suppression of Akirin1 mediates glucocorticoid-induced satellite cell dysfunction. *PLoS One* 2013; **8**: e58554.
22 Zhang L, Pan J, Dong Y, Tweardy DJ, Dong Y, Garibotto G et al. Stat3 activation Links a C/EBPdelta to myostatin pathway to stimulate loss of muscle mass. *Cell Metab* 2013; **18**: 368–379.
23 Zhang L, Du J, Hu Z, Han G, Delafontaine P, Garcia G et al. IL-6 and serum amyloid A synergy mediates angiotensin II-induced muscle wasting. *J Am Soc Nephrol* 2009; **20**: 604–612.
24 Wang Y, Huang L, Abdelrahim M, Cai Q, Truong A, Bick R et al. Stanniocalcin-1 suppresses superoxide generation in macrophages through induction of mitochondrial UCP2. *J Leukoc Biol* 2009; **86**: 981–988.
25 Zhou X, Wang JL, Lu J, Song Y, Kwak KS, Jiao Q et al. Reversal of cancer cachexia and muscle wasting by ActRIIB antagonism leads to prolonged survival. *Cell* 2010; **142**: 531–543.

26 Meng F, Lowell CA. Lipopolysaccharide (LPS)-induced macrophage activation and signal transduction in the absence of Src-family kinases Hck, Fgr, and Lyn. *J Exp Med* 1997; **185**: 1661–1670.

27 Ahima RS. Metabolic actions of adipocyte hormones: focus on adiponectin. *Obesity (Silver Spring)* 2006; **14**: 9S–15S.

28 Lihn AS, Pedersen SB, Richelsen B. Adiponectin: action, regulation and association to insulin sensitivity. *Obes Rev* 2005; **6**: 13–21.

29 Dyck DJ. Adipokines as regulators of muscle metabolism and insulin sensitivity. *Appl Physiol Nutr Metab* 2009; **34**: 396–402.

30 Leibel RL, Hirsch J. Metabolic characterization of obesity. *Ann Intern Med* 1985; **103**: 1000–1002.

31 Kahn BB, Flier JS. Obesity and insulin resistance. *J Clin Invest* 2000; **106**: 473–481.

32 Hotamisligil GS. Inflammation and metabolic disorders. *Nature* 2006; **444**: 860–867.

33 Dong Y, Lakhia R, Thomas SS, Dong Y, Wang XH, Silva KA et al. Interactions between p-Akt and Smad3 in injured muscles initiate myogenesis or fibrogenesis. *Am J Physiol Endocrinol Metab* 2013; **305**: E367–E375.

34 Sartori R, Milan G, Patron M, Mammucari C, Blaauw B, Abraham R et al. Smad2 and 3 transcription factors control muscle mass in adulthood. *Am J Physiol Cell Physiol* 2009; **296**: C1248–C1257.

35 Pan DA, Lillioja S, Kriketos AD, Milner MR, Baur LA, Bogardus C et al. Skeletal muscle triglyceride levels are inversely related to insulin action. *Diabetes* 1997; **46**: 983–988.

36 Hoppeler H, Howald H, Conley K, Lindstedt SL, Claassen H, Vock P et al. Endurance training in humans: aerobic capacity and structure of skeletal muscle. *J Appl Physiol (1985)* 1985; **59**: 320–327.

37 Dela F, Larsen JJ, Mikines KJ, Ploug T, Petersen LN, Galbo H. Insulin-stimulated muscle glucose clearance in patients with NIDDM. Effects of one-legged physical training. *Diabetes* 1995; **44**: 1010–1020.

38 Gollnick PD, Saltin B. Significance of skeletal muscle oxidative enzyme enhancement with endurance training. *Clin Physiol* 1982; **2**: 1–12.

39 Akpan I, Goncalves MD, Dhir R, Yin X, Pistilli EE, Bogdanovich S et al. The effects of a soluble activin type IIB receptor on obesity and insulin sensitivity. *Int J Obes (Lond)* 2009; **33**: 1265–1273.

40 Bernardo BL, Wachtmann TS, Cosgrove PG, Kuhn M, Opsahl AC, Judkins KM et al. Postnatal PPARdelta activation and myostatin inhibition exert distinct yet complimentary effects on the metabolic profile of obese insulin-resistant mice. *PLoS One* 2010; **5**: e11307.

41 Hamrick MW, Pennington C, Webb CN, Isales CM. Resistance to body fat gain in 'double-muscled' mice fed a high-fat diet. *Int J Obes (Lond)* 2006; **30**: 868–870.

42 Kelly DP. Medicine. Irisin, light my fire. *Sci* 2012; **336**: 42–43.

43 Stanford KI, Middelbeek RJ, Townsend KL, An D, Nygaard EB, Hitchcox KM et al. Brown adipose tissue regulates glucose homeostasis and insulin sensitivity. *J Clin Invest* 2013; **123**: 215–223.

44 Chondronikola M, Volpi E, Borsheim E, Porter C, Annamalai P, Enerback S et al. Brown adipose tissue improves whole-body glucose homeostasis and insulin sensitivity in humans. *Diabetes* 2014; **63**: 4089–4099.

45 LeBrasseur NK, Schelhorn TM, Bernardo BL, Cosgrove PG, Loria PM, Brown TA. Myostatin inhibition enhances the effects of exercise on performance and metabolic outcomes in aged mice. *J Gerontol A Biol Sci Med Sci* 2009; **64**: 940–948.

46 Murphy KT, Koopman R, Naim T, Leger B, Trieu J, Ibebunjo C et al. Antibody-directed myostatin inhibition in 21-mo-old mice reveals novel roles for myostatin signaling in skeletal muscle structure and function. *FASEB J* 2010; **24**: 4433–4442.

47 Zhang C, McFarlane C, Lokireddy S, Bonala S, Ge X, Masuda S et al. Myostatin-deficient mice exhibit reduced insulin resistance through activating the AMP-activated protein kinase signalling pathway. *Diabetologia* 2011; **54**: 1491–1501.

48 Shan T, Liang X, Bi P, Kuang S. Myostatin knockout drives browning of white adipose tissue through activating the AMPK-PGC1alpha-Fndc5 pathway in muscle. *FASEB J* 2013; **27**: 1981–1989.

49 Wang M, Yu H, Kim YS, Bidwell CA, Kuang S. Myostatin facilitates slow and inhibits fast myosin heavy chain expression during myogenic differentiation. *Biochem Biophys Res Commun* 2012; **426**: 83–88.

50 Hennebry A, Berry C, Siriett V, O'Callaghan P, Chau L, Watson T et al. Myostatin regulates fiber-type composition of skeletal muscle by regulating MEF2 and MyoD gene expression. *Am J Physiol Cell Physiol* 2009; **296**: C525–C534.

51 Girgenrath S, Song K, Whittemore LA. Loss of myostatin expression alters fiber-type distribution and expression of myosin heavy chain isoforms in slow- and fast-type skeletal muscle. *Muscle Nerve* 2005; **31**: 34–40.

52 Jorgensen SB, Richter EA, Wojtaszewski JF. Role of AMPK in skeletal muscle metabolic regulation and adaptation in relation to exercise. *J Physiol* 2006; **574/Pt 1**: 17–31.

53 Yadav H, Rane SG. TGF-beta/Smad3 Signaling Regulates Brown Adipocyte Induction in White Adipose Tissue. *Front Endocrinol (Lausanne)* 2012; **3**: 35.

54 Fournier B, Murray B, Gutzwiller S, Marcaletti S, Marcellin D, Bergling S et al. Blockade of the activin receptor IIb activates functional brown adipogenesis and thermogenesis by inducing mitochondrial oxidative metabolism. *Mol Cell Biol* 2012; **32**: 2871–2879.

55 Yadav H, Quijano C, Kamaraju AK, Gavrilova O, Malek R, Chen W et al. Protection from obesity and diabetes by blockade of TGF-beta/Smad3 signaling. *Cell Metab* 2011; **14**: 67–79.

56 Tseng YH, Kokkotou E, Schulz TJ, Huang TL, Winnay JN, Taniguchi CM et al. New role of bone morphogenetic protein 7 in brown adipogenesis and energy expenditure. *Nature* 2008; **454**: 1000–1004.

57 Schulz TJ, Huang TL, Tran TT, Zhang H, Townsend KL, Shadrach JL et al. Identification of inducible brown adipocyte progenitors residing in skeletal muscle and white fat. *Proc Natl Acad Sci USA* 2011; **108**: 143–148.

58 Koncarevic A, Kajimura S, Cornwall-Brady M, Andreucci A, Pullen A, Sako D et al. A novel therapeutic approach to treating obesity through modulation of TGFbeta signaling. *Endocrinology* 2012; **153**: 3133–3146.